ARTICLE

Unusual competition of superconductivity and charge-density-wave state in a compressed topological kagome metal

F. H. Yu[1], D. H. Ma[1], W. Z. Zhuo[1], S. Q. Liu[1], X. K. Wen[1], B. Lei[1], J. J. Ying[1✉] & X. H. Chen [1,2,3✉]

Understanding the competition between superconductivity and other ordered states (such as antiferromagnetic or charge-density-wave (CDW) state) is a central issue in condensed matter physics. The recently discovered layered kagome metal AV_3Sb_5 (A = K, Rb, and Cs) provides us a new playground to study the interplay of superconductivity and CDW state by involving nontrivial topology of band structures. Here, we conduct high-pressure electrical transport and magnetic susceptibility measurements to study CsV_3Sb_5 with the highest T_c of 2.7 K in AV_3Sb_5 family. While the CDW transition is monotonically suppressed by pressure, superconductivity is enhanced with increasing pressure up to P1 ≈ 0.7 GPa, then an unexpected suppression on superconductivity happens until pressure around 1.1 GPa, after that, T_c is enhanced with increasing pressure again. The CDW is completely suppressed at a critical pressure P2 ≈ 2 GPa together with a maximum T_c of about 8 K. In contrast to a common dome-like behavior, the pressure-dependent T_c shows an unexpected double-peak behavior. The unusual suppression of T_c at P1 is concomitant with the rapidly damping of quantum oscillations, sudden enhancement of the residual resistivity and rapid decrease of magnetoresistance. Our discoveries indicate an unusual competition between superconductivity and CDW state in pressurized kagome lattice.

[1] Hefei National Laboratory for Physical Sciences at Microscale and Department of Physics, and CAS Key Laboratory of Strongly-coupled Quantum Matter Physics, University of Science and Technology of China, Hefei, Anhui, China. [2] CAS Center for Excellence in Quantum Information and Quantum Physics, Hefei, Anhui, China. [3] Collaborative Innovation Center of Advanced Microstructures, Nanjing, PR China. ✉email: yingjj@ustc.edu.cn; chenxh@ustc.edu.cn

Superconductivity and the charge density wave (CDW) state are two different cooperative electronic states, and both of them are originated from electron–phonon coupling and Fermi surface instabilities. Superconductivity is often observed in CDW materials, however, the interplay between CDW order and superconductivity is still not well elucidated[1–5]. For example, the maximum T_c in compressed TiSe$_2$ or Cu$_x$TiSe$_2$ is reached when the CDW order is completely suppressed[2,6]; however, the superconductivity in compressed 1T-TaS$_2$ and 2H-NbSe$_2$ seems to be independent of the CDW order[7,8].

The materials with kagome lattice provide a fertile ground to study the frustrated, novel correlated, and topological electronic states owing to unusual lattice geometry[9–12]. Recently, a new family of quasi two-dimensional kagome metals AV$_3$Sb$_5$ (A = K, Rb Cs) has attracted tremendous attention[13]. These materials crystallize in the $P6/mmm$ space group, forming layers of ideal kagome nets of V ions coordinated by Sb. Besides topological properties, AV$_3$Sb$_5$ exhibits both CDW[13,14] and superconductivity[15–17]. Ultra-low temperature thermal conductivity measurements on CsV$_3$Sb$_5$ single crystal shows a finite residual linear term, implying an unconventional nodal superconductivity[18]. Intertwining the superconductivity and CDW state by involving nontrivial topology of band structures results in many exotic properties in this type of materials. For example, topological charge order was reported in KV$_3$Sb$_5$[14], signatures of spin-triplet superconductivity were claimed in Nb-K$_{1-x}$V$_3$Sb$_5$ devices[19], and unconventional giant anomalous Hall effect was observed in K$_{1-x}$V$_3$Sb$_5$ and superconducting CsV$_3$Sb$_5$[20,21]. However, the superconducting transition temperature (T_c) in this system is relatively low, and its correlation with the CDW and non-trivial topological states are still not known.

High pressure is a clean method to tune the electronic properties without introducing any impurities, and pressure is often used as a control parameter to tune superconductivity and CDW state. Here, we performed high-pressure electrical transport measurements on CsV$_3$Sb$_5$ single crystals with the highest T_c of 2.7 K in AV$_3$Sb$_5$ family. Maximum T_c of 8 K is observed at P2 ≈ 2 GPa when CDW is completely suppressed. Strikingly, an unusual suppression on superconductivity is observed between P1 ≈ 0.7 GPa and P2 ≈ 2 GPa. These results indicate an unexpected, exotic competition between CDW and superconductivity in this region, which makes CsV$_3$Sb$_5$ a rare platform to investigate the interplay of multiple electronic orders.

Results

High pressure resistivity and magnetic susceptibility measurements

We performed resistivity and magnetic susceptibility measurements on CsV$_3$Sb$_5$ under pressure to track the evolution of the CDW state and superconductivity in the compressed material. Temperature dependence of resistivity for CsV$_3$Sb$_5$ under various pressures is shown in Fig. 1. As shown in Fig. 1a, an anomaly due to the CDW transition in the resistivity[15] is clearly visible for sample 1 with PCC. The CDW transition temperature T^* gradually decreases with increasing the pressure, and the anomaly becomes much weaker at high pressures. We can determine the CDW transition temperature T^* precisely in the derivative resistivity curves as shown in Fig. 1b. The anomaly clearly shifts to lower temperatures with increasing the pressure, and disappears at the pressure of P2 ≈ 2 GPa. The anomaly of $d\rho_{xx}/dT$ at T^* gradually evolves from a broad peak to a peak-dip feature around P1. Further increasing the pressure above P1, the peak gradually weakens and the dip becomes more pronounced. The $d\rho_{xx}/dT$ anomaly is associated to the change of the band structure and electron scattering rate in the CDW state.

Therefore, such change of the shape of $d\rho_{xx}/dT$ anomaly indicates the possible change of the CDW transition around P1. To track the evolution of T_c with pressure, the low-temperature resistivity of CsV$_3$Sb$_5$ under various pressures is shown in Fig. 1c, d for sample1 with PCC and sample 2 with DAC, respectively. The T_c first increases with increasing pressure as shown in Fig. 1c, however, the superconducting transition becomes much broader with pressure larger than P1 of ~0.7 GPa, reminiscent of an inhomogeneous superconductivity in which multi superconducting phases coexists. In the high-pressure magnetic susceptibility measurements for sample 3 with PCC as shown in Supplementary Fig. 2, the superconducting transition temperature T_c^{M2} determined by the magnetic susceptibility gradually increases with increasing the pressure below P1. With the pressure above P1, the superconducting volume fraction suddenly decreases. Further increasing the pressure, the bulk superconductivity T_c^{M2} emerges below 4 K around 1.1 GPa, but the magnetic susceptibility shows a weak reduction at T_c^{M1} with higher temperature, indicating an inhomogeneous superconductivity, consistent with our resistivity measurements. It is striking that the superconducting transition becomes sharp again around P2. Meanwhile the highest T_c of 8 K is obtained. It should be addressed that the maximum T_c achieved at high pressure is 3 times higher than that (2.7 K) at ambient pressure. With further increasing the pressure, the T_c is monotonically suppressed and completely disappears above 12 GPa as shown in Fig. 1d for sample 2 with DAC. The pressure inhomogeneity or pressure induced disorder may cause the broadening of the superconducting transition. Such extrinsic effects become more pronounced with increasing the pressure. However, in our case, the superconducting transition at P2 is very sharp, which indicates that such extrinsic effect is negligible at least below P2 and the broadening of the superconducting transition between P1 and P2 is intrinsic.

Figure 2a, b shows superconducting transition under different magnetic fields for sample 1 with PCC around P1 and P2 with magnetic field applied along c axis, respectively. Much higher magnetic field is needed to suppress superconductivity around P1 and P2 compared with that at ambient pressure[15,18]. To investigate the evolution of H_{c2} under pressure, we plot H_{c2} (determined by T_c^{zero}) as a function of temperature under various pressures, as shown in Fig. 2c, d. The H_{c2} shows strong pressure dependence. H_{c2} dramatically increases with increasing the pressure, and reaches a local maximum value around P1. With further increasing the pressure, the H_{c2} can be rapidly suppressed, as shown in Fig. 2c. When the pressure reaches P2, H_{c2} dramatically increases to the maximum value, then H_{c2} can be gradually suppressed with further increasing the pressure, as shown in Fig. 2d.

Phase diagram with pressure for CsV$_3$Sb$_5$ single crystal

Combing the high-pressure electrical and magnetic susceptibility measurements on sample 1 and 3 with PCC and sample 2 with DAC, we can map out the phase diagram of CsV$_3$Sb$_5$ with pressure, as shown in Fig. 3a, b. The CDW is monotonically suppressed with increasing pressure, and the maximum T_c locates at the endpoint of CDW. A subsequent monotonic reduction of T_c is followed at higher pressure. The relatively high T_c (8 K) achieved at high pressure makes it the record in the kagome lattice materials. Such competition between CDW state and superconductivity is usual since the gap opening at CDW state would dramatically reduce the density of states at Fermi surfaces, leading to the suppression of superconductivity within Bardeen-Cooper-Schrieffer (BCS) scenario. It is striking that the superconducting transition becomes much broad with pressure
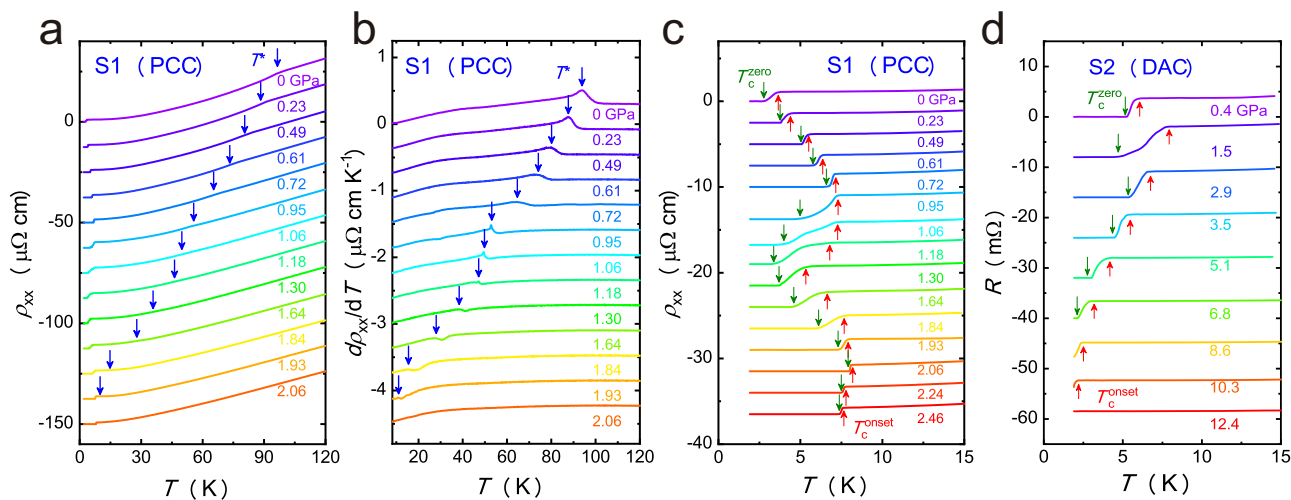
Fig. 1 Temperature dependence of resistivity in CsV$_3$Sb$_5$ single crystals under high pressure. a Temperature dependences of resistivity under various pressures for sample 1 measured with PCC. **b** The derivative $d\rho_{xx}/dT$ curves under various pressures. The blue arrows indicate the CDW transition temperature T^*. **c**, **d** The evolution of superconducting transition temperatures under pressure for sample 1 with PCC and sample 2 with DAC. The red and green arrows represent the T_c^{onset} and T_c^{zero}, respectively. All the curves were shifted vertically for clarity.
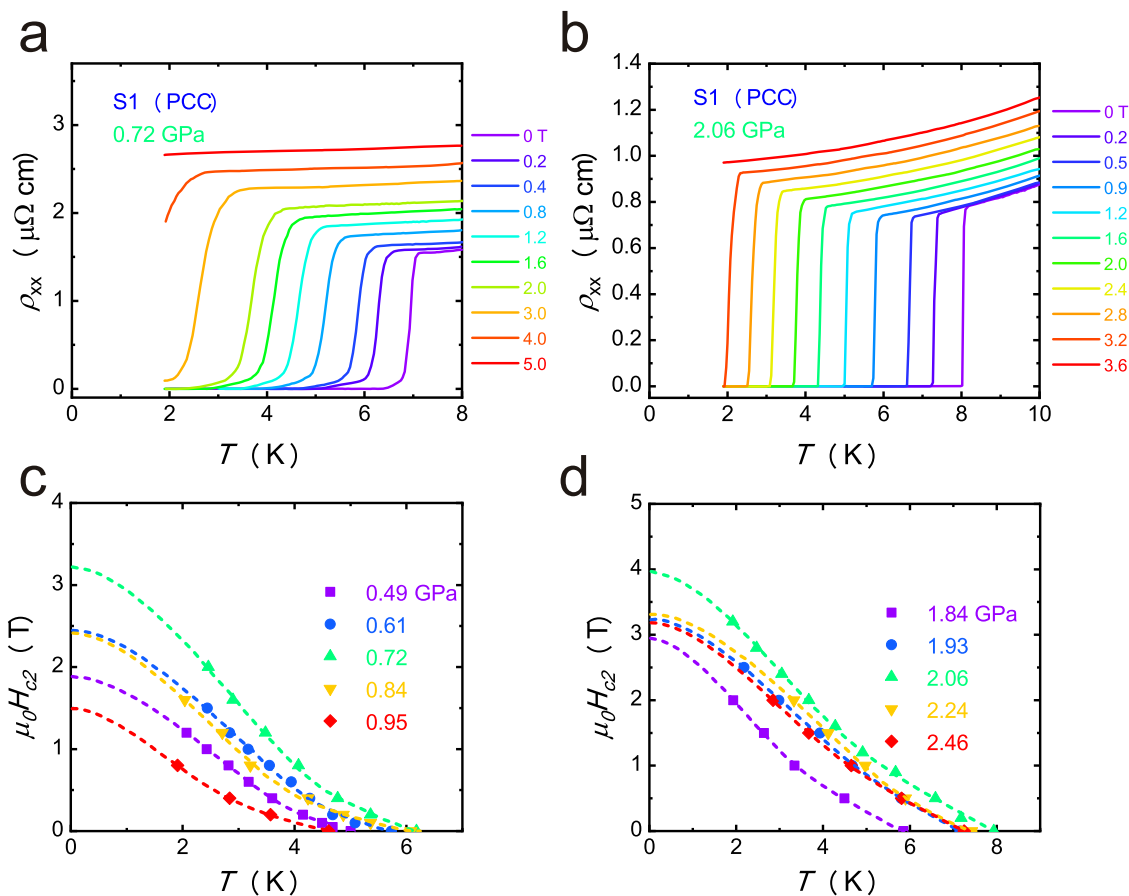
Fig. 2 Upper critical field for CsV$_3$Sb$_5$ single crystal under various pressures. Upper critical field (H_{c2}) measurements for sample1 around P1 (**a**) and P2 (**b**) with magnetic field applied along c axis. **c**, **d** The upper critical field $\mu_0 H_{c2}$ vs. T under various pressures. The dashed lines are the fitting curves by using the two-band model.

between P1 and P2, and T_c together with H_{c2} are strongly suppressed. The T^* shows a weak anomaly around P1, which suggests the transformation of CDW state. Above P1, the superconductivity shows much stronger competition with CDW order, which will be discussed later. We can estimate the H_{c2} at

zero temperature ($H_{c2}(0)$) by using the two-band model[22] of H_{c2} vs T curves as shown in Fig. 2c, d. The pressure dependence of the extracted $H_{c2}(0)$ is shown in Fig. 3c, and two peaks are clearly located at P1 and P2. The magnitude of $H_{c2}(0)$ at P1 and P2 is one order larger than that at ambient pressure.
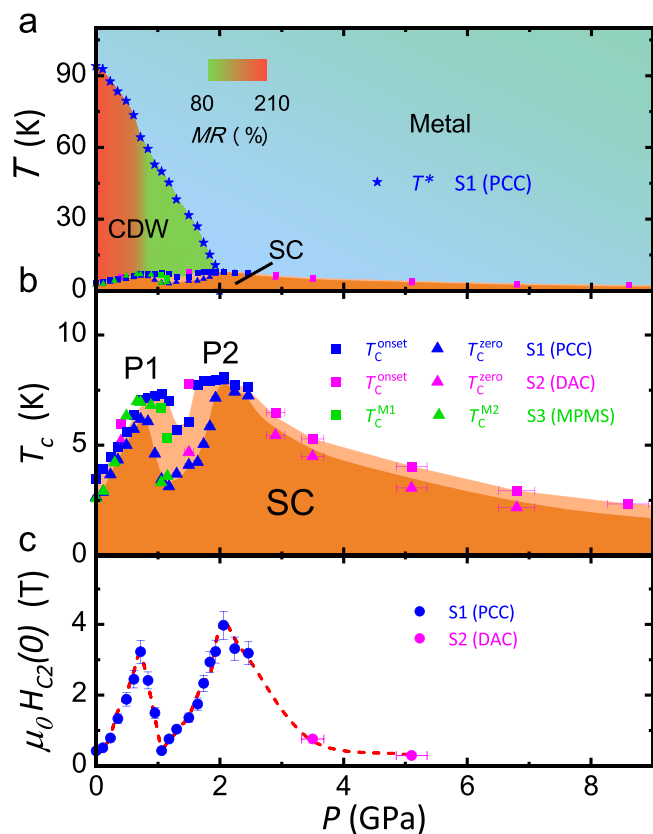
Fig. 3 Phase diagram with pressure for CsV$_3$Sb$_5$ single crystal. a Phase diagram of CsV$_3$Sb$_5$ with pressure. CDW transition temperature T^* gradually suppressed with increasing the pressure. T^* shows an anomaly around P1. The color inside the CDW phase represents the magnitude of magnetoresistance measured at 9 T and 10 K. **b** Pressure dependence of superconducting transition temperatures T_c^{onset}, T_c^{zero}, T_c^{M1} and T_c^{M2} measured on various samples. T_c is strongly suppressed with the pressure between P1 and P2. **c** Pressure dependence of upper critical field at zero temperature, two peaks can be observed at P1 and P2.

Two transitions at P1 and P2. The pressure dependence of T_c^{zero} clearly shows that two peaks are located at P1 and P2, and the superconducting transition width ΔT_c shows sudden enhancement with pressure between P1 and P2, as shown in Fig. 4a. In order to unveil the unusual suppression of superconductivity between P1 and P2, we plot the residual resistivity and residual-resistivity ratio (RRR) as a function of pressure, as shown in Fig. 4b. The residual resistivity suddenly increases around P1 and keeps at a relatively high value with the pressure between P1 and P2. Above P2, the residual resistivity suddenly drops. RRR also exhibits reduction with pressure between P1 and P2. The magnetoresistance (MR) measured under magnetic field of 9 Tesla and at the temperature of 10 K suddenly drops around P1. The MR measured at 3 T shows an anomaly at P1 and sudden drops at P2. In addition, the magnetoresistance of the low-field region at 10 K evolves from "V" shape to "U" shape at P2 as shown in Supplementary Fig. 4. Temperature dependence of MR at high pressure also evolves from "V" shape to "U" shape as shown in Supplementary Fig. 5. These results indicate that the low-field linear MR is an intrinsic property of the CDW phase, since the MR exhibits quadratic temperature-dependence when the CDW is suppressed by both of heating and pressure. However, the room-temperature resistivity gradually decreases with increasing the pressure, and does not show any anomaly at P1 and P2 as shown in Fig. 4c. These results indicate that the transitions at P1 and P2 are related to the CDW transitions rather than the

normal state change at high temperature. The Shubnikov-de Haas (SdH) quantum oscillations (QOs) measurements at 2 K exhibit a rapid damping above P1 as shown in Supplementary Fig. 6, which is possibly associated to the enhancement of scattering rate for the resolved four bands, providing evidence for a transformation of the CDW state at P1.

Discussion

Although superconductivity was reported in some kagome lattice materials[23,24], the previously reported T_c is quite low. Our high-pressure work demonstrates that the T_c in this V-based kagome material can be relatively high and easily tuned. Further enhancement of T_c should be possible in this type of materials by using the other methods to destroy the CDW state, such as chemical substitution or electrical gating. The maximum T_c locates at the endpoint of CDW, which resembles many other CDW materials[2,6], indicating the competition between superconductivity and CDW state. The most interesting discovery in this work is the region between P1 and P2, in which the CDW and superconductivity have much stronger competition, leading to the dramatical suppression of T_c and increment of superconducting transition width (ΔT_c). In addition, the sudden enhancement of residual resistivity and damping of QOs indicate a transition at P1, possibly due to the formation of a new CDW state. One possibility is that the original modulation pattern may change under pressure, and a new commensurate CDW (CCDW) state or an incommensurate CDW (ICCDW) state emerges above P1. Pressure-induced CCDW to ICCDW transition has been observed in the 2H-TaSe$_2$[25]. Such phase transition will dramatically modify the Fermi surface and alters T_c. However, it cannot explain the superconducting transition broadening after phase transition. Another possibility is that a nearly commensurate CDW (NCCDW) state forms above P1, in which CDW domains are separated by domain walls (DW). Similar transition was also observed in 1T-TaS$_2$ with increasing the temperature[26]. It is proposed a tri-hexagonal (inverse Star of David) modulation pattern shows up in the CCDW state for AV$_3$Sb$_5$[14]. In the NCCDW state, the charge may transfer to the narrow DWs since CDW domains are partially gapped[27]. The enhanced interaction and scattering at the DW network will lead to the higher resistivity[27]. The superconductivity in the CDW domains may be strongly suppressed due to the reduction of carrier density, however, the superconductivity in the DWs may have higher T_c, leading to the inhomogeneous superconductivity. To be reminded, the rather broad superconducting transition in the NCCDW state actually resembles the manifestation of so-called pair-density-wave (PDW) order in high-T_c cuprate superconductors[28]. In La$_{2-x}$Ba$_x$CuO$_4$, superconductivity is greatly suppressed around 1/8 doping level due to the formation of a long-ranged stripe order and the final superconducting state at low temperatures is attributed to a PDW order[29–31]. This is very similar to our cases around the region with unusual suppression of T_c. Therefore, it is speculated that a similar PDW order might also emerge in the superconducting state between P1 and P2, which needs further evidences from spatial-resolved spectroscopy. Our discoveries may help to clarify the origin of similar behaviors observed in other systems with competing orders. In fact, two-dome T_c behavior were also observed in some superconductors[32–34], which might be a general feature for superconductors with competing density waves. However, we would like to note that two-dome SC behavior in CsV$_3$Sb$_5$ occurs within the CDW phase, which is different with the other systems where a second SC dome appears when the density wave order is completely suppressed. Quantum critical behavior can emerge at the endpoint of CDW order[35]. In order to search for the quantum criticality in this system, we analysis the low-temperature resistivity, as shown in Supplementary Fig. 8. Above P2, the low-temperature resistivity
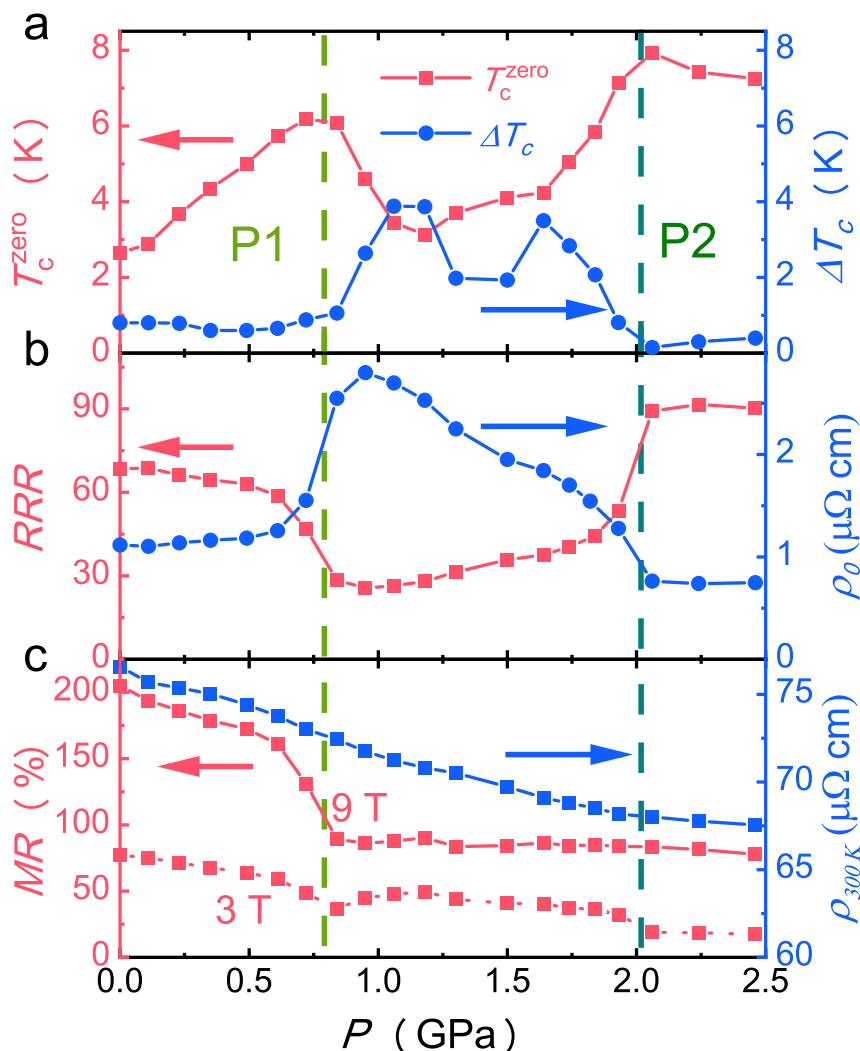
Fig. 4 Pressure dependence of residual resistivity, residual-resistivity ratio and magnetoresistance for CsV$_3$Sb$_5$ single crystal. a Pressure dependence of T_c^{zero} and ΔT_c for sample 1 with PCC. T_c^{zero} exhibits two peaks at P1 and P2. **b** Pressure dependence of residual resistivity and residual resistivity ratio (RRR) for sample 1 with PCC. **c** Pressure dependence of magnetoresistance (9 T and 3 T, 10 K) and room-temperature resistivity.

follows T^2 behavior below 35 K, therefore our current results do not support the existence of quantum fluctuations around P2. However, ultralow-temperature experiments are still highly required to clarify possible quantum criticality at lower temperature.

In conclusion, we systematically investigate the high-pressure transport and magnetic susceptibility properties of the newly discovered topological kagome metal CsV$_3$Sb$_5$. When CDW is completely suppressed, the maximum T_c up to 8 K can be reached, and is three times higher than that (2.7 K) at ambient pressure. More interestingly, superconductivity shows an unusual suppression with pressure between P1 and P2. A transformation of CDW state occurs above P1 accompanied with the rapidly damping of QOs, sudden enhancement of residual resistivity and the rapid decrease of magnetoresistance.

Methods

Material syntheses. Single crystals of CsV$_3$Sb$_5$ were synthesized via a self-flux growth method similar to the previous reports[15]. In order to prevent the reaction of Cs with air and water, all the preparation processes were performed in an argon glovebox. After reaction in the furnace, the as-grown CsV$_3$Sb$_5$ single crystals are stable in the air. The excess flux is removed using water and millimeter-sized single crystal can be obtained.

High-pressure measurements. Piston cylinder cell (PCC) was used to generate hydrostatic pressure up to 2.4 GPa for high-pressure electrical transport measurements. Daphne 7373 was used as the pressure transmitting medium in PCC. The pressure values in PCC were determined from the superconducting transition of Sn[36]. Diamond anvil cell (DAC) was used to generate the pressure up to 12 GPa. Diamond anvils with 500 μm culet and c-BN gasket with sample chambers of diameter 200 μm were used. Four Pt wires were adhered to the sample and NaCl was used as the pressure transmitting medium. Pressure was calibrated by using the ruby fluorescence shift at room temperature[37]. Electrical transport measurements were carried out in a Quantum Design physical property measurement system. High-pressure magnetic susceptibility measurements were performed in a miniature PCC using a SQUID magnetometer (MPMS-5 T, Quantum Design).

Note added: During the preparation of this manuscript, we noticed a similar high-pressure work[38].

References

1. Gabovich, A. M., Voitenko, A. I., Annett, J. F. & Ausloos, M. Charge- and spin-density-wave superconductors. *Superconductor Sci. Technol.* **14**, R1–R27 (2001).

2. Kusmartseva, A. F., Sipos, B., Berger, H., Forró, L. & Tutiš, E. Pressure induced superconductivity in pristine 1T-TiSe$_2$. *Phys. Rev. Lett.* **103**, 236401 (2009).

3. Joe, Y. I. et al. Emergence of charge density wave domain walls above the superconducting dome in 1T-TiSe$_2$. *Nat. Phys.* **10**, 421–425 (2014).

4. Johannes, M. D. & Mazin, I. I. Fermi surface nesting and the origin of charge density waves in metals. *Phys. Rev. B* **77**, 165135 (2008).

5. Zhu, X., Cao, Y., Zhang, J., Plummer, E. W. & Guo, J. Classification of charge density waves based on their nature. *Proc. Natl Acad. Sci. USA* **112**, 2367–2371 (2015).

6. Morosan, E. et al. Superconductivity in Cu$_x$TiSe$_2$. *Nat. Phys.* **2**, 544–550 (2006).

7. Sipos, B. et al. From Mott state to superconductivity in 1T-TaS 2. *Nat. Mater.* **7**, 960–965 (2008).

8. Feng, Y. et al. Order parameter fluctuations at a buried quantum critical point. *Proc. Natl Acad. Sci. USA* **109**, 7224–7229 (2012).

9. Zhou, Y., Kanoda, K. & Ng, T.-K. Quantum spin liquid states. *Rev. Mod. Phys.* **89**, 025003 (2017).

10. Han, T.-H. et al. Fractionalized excitations in the spin-liquid state of a kagome-lattice antiferromagnet. *Nature* **492**, 406–410 (2012).

11. Sachdev, S. Kagome- and triangular-lattice Heisenberg antiferromagnets: Ordering from quantum fluctuations and quantum-disordered ground states with unconfined bosonic spinons. *Phys. Rev. B* **45**, 12377–12396 (1992).

12. Mazin, I. I. et al. Theoretical prediction of a strongly correlated Dirac metal. *Nat. Commun.* **5**, 4261 (2014).

13. Ortiz, B. R. et al. New kagome prototype materials: discovery of KV$_3$Sb$_5$, RbV$_3$Sb$_5$, and CsV$_3$Sb$_5$. *Phys. Rev. Mater.* **3**, 094407 (2019).

14. Jiang, Y.-X. et al. Discovery of topological charge order in kagome superconductor KV$_3$Sb$_5$. Preprint at http://arxiv.org/abs/2012.15709 (2020).

15. Ortiz, B. R. et al. CsV$_3$Sb$_5$: A Z_2 Topological Kagome Metal with a Superconducting Ground State. *Phys. Rev. Lett.* **125**, 247002 (2020).

16. Ortiz, B. R. et al. Superconductivity in the Z_2 kagome metal KV$_3$Sb$_5$. *Phys. Rev. Materials* **5**, 034801 (2021).

17. Yin, Q. et al. Superconductivity and normal-state properties of kagome metal RbV$_3$Sb$_5$ single crystals. *Chin. Phys. Lett.* **38**, 037403 (2021).

18. Zhao, C. C. et al. Nodal superconductivity and superconducting dome in the topological Kagome metal CsV$_3$Sb$_5$. Preprint at http://arxiv.org/abs/2102.08356 (2021).

19. Wang, Y. et al. Proximity-induced spin-triplet superconductivity and edge supercurrent in the topological Kagome metal, K$_{1-x}$V$_3$Sb$_5$. Preprint at http://arxiv.org/abs/2012.05898 (2020).

20. Yang, S.-Y. et al. Giant, unconventional anomalous Hall effect in the metallic frustrated magnet candidate, KV$_3$Sb$_5$. *Sci. Adv.* **6**, eabb6003 (2020).

21. Yu, F. H. et al. Concurrence of anomalous Hall effect and charge density wave in a superconducting topological kagome metal. Preprint at http://arxiv.org/abs/2102.10987 (2021).

22. Gurevich, A. Enhancement of the upper critical field by nonmagnetic impurities in dirty two-gap superconductors. *Phys. Rev. B* **67**, 184515 (2003).

23. Li, S., Xing, J., Tao, J., Yang, H. & Wen, H.-H. Superconductivity in Ba$_{2/3}$Pt$_3$B$_2$ with the Kagome lattice. *Ann. Phys.* **358**, 248–254 (2015).

24. Yu, F. H. et al. Pressure-induced superconductivity in a shandite compound Pd$_3$Pb$_2$Se$_2$ with the Kagome lattice. *N. J. Phys.* **22**, 123013 (2020).

25. McWhan, D. B., Fleming, R. M., Moncton, D. E. & DiSalvo, F. J. Reentrant lock-in transition of the charge-density wave in 2H-TaSe$_2$ at high pressure. *Phys. Rev. Lett.* **45**, 269–272 (1980).

26. Wilson, J. A., Di Salvo, F. J. & Mahajan, S. Charge-density waves and superlattices in the metallic layered transition metal dichalcogenides. *Adv. Phys.* **24**, 117–201 (1975).

27. Lee, K. et al. Metal-to-insulator transition in Pt-doped TiSe$_2$ driven by emergent network of narrow transport channels. *npj Quantum Mater.* **6**, 8 (2021).

28. Keimer, B., Kivelson, S. A., Norman, M. R., Uchida, S. & Zaanen, J. From quantum matter to high-temperature superconductivity in copper oxides. *Nature* **518**, 179–186 (2015).

29. Agterberg, D. F. et al. The physics of pair-density waves: cuprate superconductors and beyond. *Annu. Rev. Condens. Matter Phys.* **11**, 231–270 (2020).

30. Li, Q., Hücker, M., Gu, G. D., Tsvelik, A. M. & Tranquada, J. M. Two-dimensional superconducting fluctuations in stripe-ordered La$_{1.875}$Ba$_{0.125}$CuO$_4$. *Phys. Rev. Lett.* **99**, 067001 (2007).

31. Hücker, M. et al. Stripe order in superconducting La$_{2-x}$Ba$_x$CuO$_4$ (0.095 < x < 0.155). *Phys. Rev. B* **83**, 104506 (2011).

32. Iimura, S. et al. Two-dome structure in electron-doped iron arsenide superconductors. *Nat. Commun.* **3**, 943 (2012).

33. Yajima, T. et al. Two superconducting phases in the isovalent solid solutions BaTi$_2$Pn$_2$O (Pn = As, Sb, and Bi). *J. Phys. Soc. Jpn.* **82**, 033705 (2013).

34. Bhoi, D. et al. Interplay of charge density wave and multiband superconductivity in 2H-Pd$_x$TaSe$_2$. *Sci. Rep.* **6**, 24068 (2016).

35. Gruner, T. et al. Charge density wave quantum critical point with strong enhancement of superconductivity. *Nat. Phys.* **13**, 967–972 (2017).

36. Jennings, L. D. & Swenson, C. A. Effects of pressure on the superconducting transition temperatures of Sn, In, Ta, Tl, and Hg. *Phys. Rev.* **112**, 31–43 (1958).

37. Mao, H. K., Xu, J. & Bell, P. M. Calibration of the ruby pressure gauge to 800 kbar under quasi-hydrostatic conditions. *J. Geophys. Res.: Solid Earth* **91**, 4673–4676 (1986).

38. Chen, K. Y. et al. Double superconducting dome and triple enhancement of Tc in the kagome superconductor CsV$_3$Sb$_5$ under high pressure. Preprint at http://arxiv.org/abs/2102.09328 (2021).

Author contributions
X.H.C. and J.J.Y. conceived and designed the experiments. F.H.Y. performed high-pressure electrical transport measurements with the assistance from J.J.Y., D.H.M., W.Z.Z., S.Q.L., X.K.W., and B.L. F.H.Y. synthesized the CsV$_3$Sb$_5$ single crystal. J.J.Y., F.H.Y., and X.H.C. analyzed and interpreted the data. J.J.Y. and X.H.C. wrote the manuscript. All authors discussed the results and commented on the manuscript.

Competing interests
The authors declare no competing interests.

Additional information
Supplementary information The online version contains supplementary material available at https://doi.org/10.1038/s41467-021-23928-w.

Correspondence and requests for materials should be addressed to J.J.Y. or X.H.C.

Peer review information *Nature Communications* thanks Pavel Volkov and the other, anonymous, reviewer(s) for their contribution to the peer review of this work. Peer reviewer reports are available.

Reprints and permission information is available at http://www.nature.com/reprints

Publisher's note Springer Nature remains neutral with regard to jurisdictional claims in published maps and institutional affiliations.